NRL Report 8002

Impedance-Match and Element-Pattern Constraints for Finite Arrays

WALTER K. KAHN

Airborne Radar Branch
Radar Division

June 16, 1976

NAVAL RESEARCH LABORATORY
Washington, D.C.

Approved for public release; distribution unlimited.

SECURITY CLASSIFICATION OF THIS PAGE (When Data Entered)

REPORT DOCUMENTATION PAGE

1. REPORT NUMBER
NRL Report 8002

2. GOVT ACCESSION NO.

3.

4. TITLE (and Subtitle)
IMPEDANCE-MATCH AND ELEMENT-PATTERN CONSTRAINTS FOR FINITE ARRAYS

5. TYPE OF REPORT & PERIOD COVERED
Interim report on a continuing NRL Problem

6. PERFORMING ORG. REPORT NUMBER

7. AUTHOR(s)
Walter K. Kahn

8. CONTRACT OR GRANT NUMBER(s)

9. PERFORMING ORGANIZATION NAME AND ADDRESS
Naval Research Laboratory
Washington, D.C. 20375

10. PROGRAM ELEMENT, PROJECT, TASK AREA & WORK UNIT NUMBERS
NRL Problem 53R02-29
Project WF12-141-601, 62712N

11. CONTROLLING OFFICE NAME AND ADDRESS
Department of the Navy
Naval Air Systems Command
Washington, D.C. 20361

12. REPORT DATE
June 16, 1976

13. NUMBER OF PAGES
35

14. MONITORING AGENCY NAME & ADDRESS(if different from Controlling Office)

15. SECURITY CLASS. (of this report)
Unclassified

15a. DECLASSIFICATION/DOWNGRADING SCHEDULE

16. DISTRIBUTION STATEMENT (of this Report)
Approved for public release; distribution unlimited.

17. DISTRIBUTION STATEMENT (of the abstract entered in Block 20, if different from Report)

18. SUPPLEMENTARY NOTES

19. KEY WORDS (Continue on reverse side if necessary and identify by block number)

Antennas	Antenna impedance
Arrays	Active impedance
Antenna feeds	Feed networks

20. ABSTRACT (Continue on reverse side if necessary and identify by block number)

It is shown how an N-element antenna array may in principle be impedance matched by means of a specially designed interconnecting feed network to N real generators (for arbitrary excitation of these generators). The resulting element patterns for a single excited element (a single generator) in the terminated-array environment are then calculated.

(Continued)

DD FORM 1 JAN 73 1473 EDITION OF 1 NOV 65 IS OBSOLETE
S/N 0102-014-6601

SECURITY CLASSIFICATION OF THIS PAGE (When Data Entered)

20. ABSTRACT (Continued)

It is shown that for closely spaced regular arrays a condition of partial match, as contrasted with perfect match for all excitations, is the more appropriate design objective. The theory is illustrated through application to a uniform array of line sources. Element patterns obtained with an appropriately matched finite array are compared with those from the corresponding matched infinite-array model, the latter patterns having been obtained previously by an independent technique. The range of finite-array parameters to which the infinite-array model approximately applies is discussed.

CONTENTS

INTRODUCTION 1

NETWORK PRELIMINARIES 2

Connections and Port Normalization Numbers 2
Representations of the Scattering Matrix and Scattering-Transfer Matrix 4

EIGENWAVE ANALYSIS OF ARRAYS 9

Uniform Versus General Arrays 9
Twofold Symmetry Analysis 9

CALCULATION OF ELEMENT PATTERNS FOR SUITABLY MATCHED ARRAYS 14

Excitation and the Radiation Fields 14
The Modified Array 16
Matching Network for the Modified Linear Array 17
Partial Match of the Array 21

APPLICATION AND EXAMPLES 22

DISCUSSION AND CONCLUSIONS 28

ACKNOWLEDGMENTS 29

REFERENCES 29

APPENDIX A — Element Patterns of a Matched Infinite Array . . 31

IMPEDANCE-MATCH AND ELEMENT-PATTERN CONSTRAINTS FOR FINITE ARRAYS

INTRODUCTION

This report deals with an investigation of mutual coupling in finite and general antenna arrays. The cost of large phased arrays and the need to make arrays conform to streamlined contours have stimulated interest in arrays of modest size. On the other hand the simplicity of the infinite-array model is so attractive, particularly in the case of regular arrays, that the lower bound on the size of arrays for which this model may be usefully applied is of great practical importance. The element pattern for a single excited element of an infinite array (in the presence of the remaining elements terminated by loads) is given by the classic formulas of Allen [1] and Hannan [2,3]. The limiting form of the element pattern resulting when such an array is matched in impedance as a phased array at all scan angles was given by Wasylkiwskyj and Kahn [4]. Here the limiting form of the element pattern is obtained by direct calculation for finite arrays of general configuration. For regular arrays, results obtained for the finite array confirm the lower bounds on array size obtained from considerations of efficiency in finite-excited infinite arrays [5]. The infinite array closely models interior elements of arrays larger than 25 elements along any diameter.

Good impedance match over a wide range of excitations for all scan angles is frequently claimed, at least as a design objective, for an array antenna. A technique is developed in the following for predicting the element patterns which would result if any given array of antennas were appropriately matched in impedance by means of a lossless feed network designed for this purpose. When the requirement for match is most broadly interpreted, namely, as match for *all* excitations, the form of our result can be anticipated from the conservation of energy [6].

Consider an array of N antennas as a dissipative N-port with input impedance matrix $Z = R + jX$. Assume the existence of a lossless $2N$-port which, if inserted between the array and N generators with unit internal impedance, will have the unit matrix as its input impedance matrix. Designating the column matrix of currents at the antenna ports by $\hat{\mathsf{I}}$ and that at the input to the matching network by I, the conservation of energy implies $\mathsf{I}^\dagger \mathsf{I} = \hat{\mathsf{I}}^\dagger R \hat{\mathsf{I}}$. The superscript $\dagger$ denotes the complex-conjugate transpose matrix. The lossless $2N$-port must therefore effect the transformation $\hat{\mathsf{I}} = R^{-1/2}\mathsf{I}$. The element patterns of the array, matched for *all* excitations, may be computed from these currents. The existence of a matching network was demonstrated by Bergfried [7] and Bergfried and Kahn [8]. The analysis and computational results presented here are based on a more convenient network structure.

Generally impedance match for *all* excitations does not constitute an appropriate objective. This distinction between match for all excitations and an appropriate partial

Manuscript submitted March 29, 1976.

match is essential in the application of this method to closely spaced arrays. For such arrays the indiscriminate requirement of match for all excitations leads to difficulties in tuning and excitation (and in computation) akin to those associated with supergain [9]. The excitations and element patterns derived using partial matching are not simply predicted by the conservation of energy.

A uniform linear array of infinite line sources will be used to illustrate the general theoretical results. Since the elements have infinite extent, this array must be considered as a special case of a planar array; it is the simplest example of such an array. When the computational results for closely spaced elements are studied, the effect of using an appropriate partial match, as opposed to one for *all* excitations, is apparent. The element patterns derived for appropriately matched finite arrays will be compared with those of an infinite array (the limiting case) obtained by an independent technique.

NETWORK PRELIMINARIES

Connections and Port Normalization Numbers

The desired excitation of a given array of antennas will be supplied from generators with finite internal impedance through a lossless feed network. It is convenient to be able to view this interconnection either in terms of voltages and currents or alternatively in terms of incident and reflected waves. In this section some aspects of the interconnection process will be reviewed [10].

The interconnection of two 2-ports is shown in Fig. 1. In terms of voltage and currents with polarities and directions shown in the diagram this interconnection clearly requires

$$V = V' , \tag{1a}$$

$$I = -I' . \tag{1b}$$

From the diagram it would appear just as clearly for incident and reflected wave amplitudes a and b that

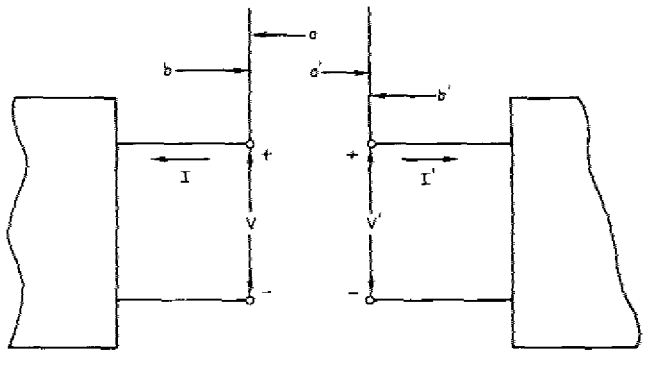

Fig. 1—Interconnection of two 2-ports

$$a = b' , \tag{2a}$$

$$b = a' . \tag{2b}$$

However, when these incident and reflected wave quantities are defined with respect to complex normalization numbers, the defining relations being

$$2a\sqrt{R_g} = V + Z_g I , \tag{3a}$$

$$2b\sqrt{R_g} = V - Z_g^* I , \tag{3b}$$

the relations (2) must be viewed with some caution.

Figure 2 presents the physical interpretation of the defining relation (3a). When $E_g = 2a\sqrt{R_g}$, this relation is the Kirchhoff-loop equation for the circuit shown. Evidently Z must have the value $Z = V/I$. The average power transferred from the generator into Z is, algebraically,

$$P = \mathrm{Re}\,(V^* I) = |a|^2 - |b|^2 . \tag{4}$$

Thus maximum power is transferred to Z when $b = 0$. From Eq. (3b) this implies

$$\frac{V}{I} = Z_g^* = Z \tag{5}$$

in agreement with the principle of conjugate impedance match.

Let us now check the consistency of relations (1) and (2). Direct substitution in (3) yields

$$2b'\sqrt{R_g} = V' - Z_g I' , \tag{6a}$$

$$2a'\sqrt{R_g} = V' + Z_g^* I' . \tag{6b}$$

These relations are of the same form as (3) except that Z_g^* replaces Z_g. That is, the "evident" interconnection relations (2) hold only when the complex normalization numbers Z_g and Z_g' are understood to be *complex conjugates* of one another.

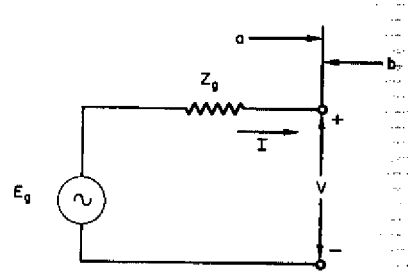

Fig. 2—Equivalent circuit for interpretation of normalization numbers Z_g

In the sequel it will be assumed that the port normalization numbers Z_g are either real or that (when an identification such as b' with a is made) the appropriate conjugate relation between the normalization numbers Z_g is maintained.

Representations of the Scattering Matrix and Scattering-Transfer Matrix

The scattering matrix relates incident and reflected wave amplitudes. Corresponding with an impedance matrix Z,

$$2R_g^{1/2}\mathbf{b} = (\mathbf{V} - Z_g^*\mathbf{I}) = (Z - Z_g^*)\mathbf{I}\,, \tag{7a}$$

$$2R_g^{1/2}\mathbf{a} = (\mathbf{V} + Z_g\mathbf{I}) = (Z + Z_g)\mathbf{I}\,. \tag{7b}$$

One eliminating $\mathbf{I}$

$$2R_g^{1/2}\mathbf{b} = (Z - Z_g^*)(Z + Z_g)^{-1}2R_g^{1/2}\mathbf{a}$$

or

$$\begin{aligned}\mathbf{b} &= \left[R_g^{-1/2}(Z - Z_g^*)(Z + Z_g)^{-1}R_g^{1/2}\right]\mathbf{a}\\ &= R_g^{-1/2}\left[1 - 2R_g(Z + Z_g)^{-1}\right]R_g^{1/2}\mathbf{a}\\ &= \left[1 - 2R_g^{1/2}(Z + Z_g)^{-1}R_g^{1/2}\right]\mathbf{a}\,.\end{aligned}$$

The scattering matrix

$$\begin{aligned}S &= R_g^{-1/2}(Z - Z_g^*)(Z + Z_g)^{-1}R_g^{1/2}\\ &= 1 - 2R_g^{1/2}(Z + Z_g)^{-1}R_g^{1/2}\end{aligned} \tag{8}$$

is symmetric if Z is symmetric, as is most easily seen from the second form of (8).

Consider the $2N$-port network shown in Fig. 3. The incident and reflected wave amplitudes are ordered into column vectors $\mathbf{a}$ and $\mathbf{b}$, so that

$$\mathbf{a} = \begin{pmatrix}\mathbf{a}_\alpha\\ \hline \mathbf{a}_\beta\end{pmatrix} \quad \text{and} \quad \mathbf{b} = \begin{pmatrix}\mathbf{b}_\alpha\\ \hline \mathbf{b}_\beta\end{pmatrix}, \tag{9a}$$

where

$$\tilde{\mathbf{a}}_\alpha = [a_1\ a_2\ \dots\ a_N] \tag{9b}$$

and

$$\tilde{\mathbf{a}}_\beta = [a_{N+1}\ a_{N+2}\ \dots\ a_{2N}]\,, \tag{9c}$$

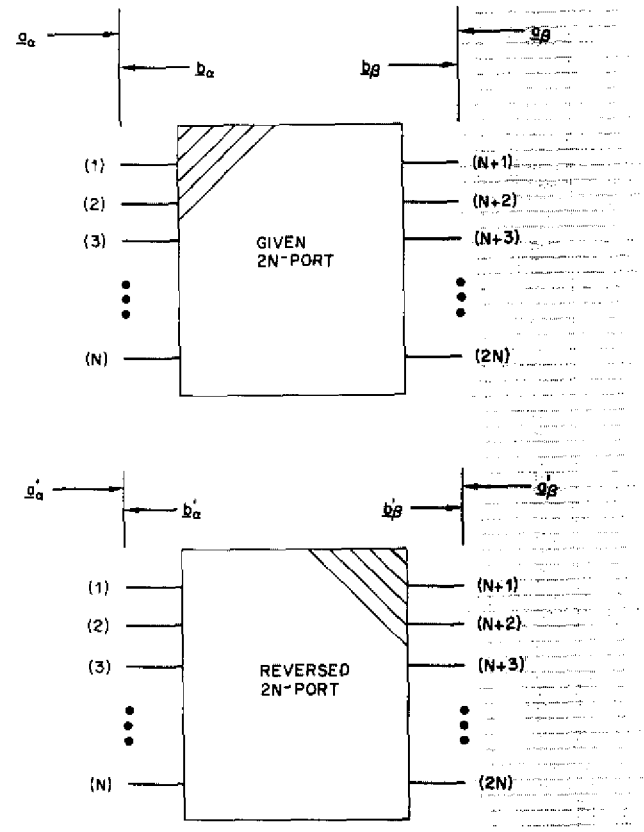

Fig. 3—The reversed $2N$-port

in which $\tilde{\mathbf{a}}_\alpha$ and $\tilde{\mathbf{a}}_\beta$ denote the row vectors which are the transpose of the column vectors $\mathbf{a}_\alpha$ and $\mathbf{a}_\beta$ respectively, and where $\tilde{\mathbf{b}}_\alpha$ and $\tilde{\mathbf{b}}_\beta$ denote similar row vectors. Then

$$\mathbf{b} = \begin{pmatrix} \mathbf{b}_\alpha \\ \hline \mathbf{b}_\beta \end{pmatrix} = \left(\begin{array}{c|c} S_{\alpha\alpha} & S_{\alpha\beta} \\ \hline S_{\beta\alpha} & S_{\beta\beta} \end{array}\right) \begin{pmatrix} \mathbf{a}_\alpha \\ \hline \mathbf{a}_\beta \end{pmatrix} = S\mathbf{a} \,. \tag{10}$$

A $2N$-port closely related to S is the reversed $2N$-port, that is, the $2N$-port obtained when the network is turned around (physically, as is often possible) *leaving port designations fixed in place*. Thus old port 1 becomes new port $N + 1$, etc. (Of course, if the port designations are kept fixed, attached to the network, the scattering matrix cannot change when the network is moved.)

It follows that the scattering matrix of the new network may be inferred from (10). The new column vectors $\mathbf{a}'$ and $\mathbf{b}'$ are

$$\mathbf{b}' = \begin{pmatrix} b'_\alpha \\ \hline b'_\beta \end{pmatrix} = \begin{pmatrix} b_\beta \\ \hline b_\alpha \end{pmatrix} = \mathcal{R}\,\mathbf{b} \tag{11a}$$

and

$$\mathbf{a}' = \left(\begin{array}{c} \mathbf{a}'_\alpha \\ \hline \mathbf{a}'_\beta \end{array}\right) = \left(\begin{array}{c} \mathbf{a}_\beta \\ \hline \mathbf{a}_\alpha \end{array}\right) = \mathcal{R}\mathbf{a}\,, \tag{11b}$$

where

$$\mathcal{R} = \left(\begin{array}{c|c} 0 & 1 \\ \hline 1 & 0 \end{array}\right).$$

Hence $\mathbf{b} = S\mathbf{a}$ implies $\mathbf{b}' = \mathcal{R}S\mathcal{R}^{-1}\mathbf{a}'$ or

$$S' = \mathcal{R}S\mathcal{R}^{-1} = \left(\begin{array}{c|c} S_{\beta\beta} & S_{\beta\alpha} \\ \hline S_{\alpha\beta} & S_{\alpha\alpha} \end{array}\right). \tag{12}$$

Note that in this instance

$$\mathcal{R}^{-1} = \left(\begin{array}{c|c} 0 & 1 \\ \hline 1 & 0 \end{array}\right) = \mathcal{R}\,. \tag{13}$$

Attention is now turned to the scattering-transfer matrix. The scattering-transfer matrix of a given $2N$-port relates the amplitudes $\mathbf{a}_\alpha$ and $\mathbf{b}_\alpha$ with $\mathbf{a}'_\alpha$ and $\mathbf{b}'_\alpha$ (rather than $\mathbf{a}_\alpha$ and $\mathbf{b}_\alpha$ with $\mathbf{a}_\beta$ and $\mathbf{b}_\beta$), where now $\mathbf{a}'_\alpha$ and $\mathbf{b}'_\alpha$ are amplitudes associated with ports 1 through N of a *succeeding* $2N$-port connected to the given $2N$-port at ports $N + 1$ through $2N$. This is illustrated in Fig. 4. The scattering-transfer matrix T_s may also be found in terms of the elements of S. By definition

$$\left(\begin{array}{c} \mathbf{a}'_\alpha \\ \hline \mathbf{b}'_\alpha \end{array}\right) = T_S \left(\begin{array}{c} \mathbf{a}_\alpha \\ \hline \mathbf{b}_\alpha \end{array}\right), \tag{14}$$

and from (10) and Fig. 4

$$\left(\begin{array}{c} \mathbf{a}'_\alpha \\ \hline \mathbf{b}'_\alpha \end{array}\right) = \left(\begin{array}{c} \mathbf{b}_\beta \\ \hline \mathbf{a}_\beta \end{array}\right) = \left(\begin{array}{c|c} S_{\beta\alpha} & S_{\beta\beta} \\ \hline 0 & 1 \end{array}\right) \left(\begin{array}{c} \mathbf{a}_\alpha \\ \hline \mathbf{a}_\beta \end{array}\right) \tag{15a}$$

and

$$\left(\begin{array}{c} \mathbf{a}_\alpha \\ \hline \mathbf{b}_\beta \end{array}\right) = \left(\begin{array}{c|c} 1 & 0 \\ \hline S_{\alpha\alpha} & S_{\alpha\beta} \end{array}\right) \left(\begin{array}{c} \mathbf{a}_\alpha \\ \hline \mathbf{a}_\beta \end{array}\right). \tag{15b}$$

The scattering-transfer matrix is obtained on eliminating $\mathbf{a}$ from the above,

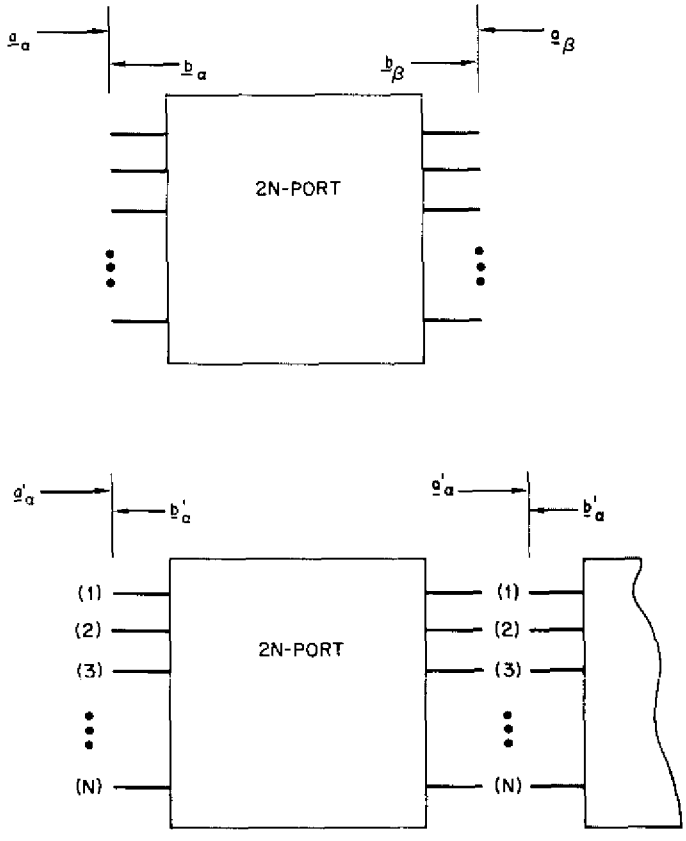

Fig. 4—Conventions for scattering-transfer representation

$$T_S = \left(\begin{array}{c|c} S_{\beta\alpha} & S_{\beta\beta} \\ \hline 0 & 1 \end{array}\right) \left(\begin{array}{c|c} 1 & 0 \\ \hline S_{\alpha\alpha} & S_{\alpha\beta} \end{array}\right)^{-1}$$

$$= \left(\begin{array}{c|c} S_{\beta\alpha} - S_{\beta\beta}S_{\alpha\beta}^{-1}S_{\alpha\alpha} & S_{\beta\beta}S_{\alpha\beta}^{-1} \\ \hline -S_{\alpha\beta}^{-1}S_{\alpha\alpha} & S_{\alpha\beta}^{-1} \end{array}\right). \tag{15c}$$

In the important special case $S_{\alpha\alpha} = S_{\beta\beta} = 0$,

$$T_S = \left(\begin{array}{c|c} S_{\beta\alpha} & 0 \\ \hline 0 & S_{\alpha\beta}^{-1} \end{array}\right). \tag{16}$$

When such a network is lossless and reciprocal, the scattering matrix being therefore unitary and symmetric,

$$S_{\alpha\beta} = \widetilde{S}_{\beta\alpha} = S_{\beta\alpha}^{-1*} . \tag{17}$$

An appropriate interconnection of ideal transformers leads to a purely real scattering matrix $S_{\alpha\beta} = S_{\beta\alpha}^{-1}$. It follows that such a network is "undone" by cascade connection with its reverse; that is,

$$T_S T_{\Re S \Re} = 1 \tag{18}$$

when $S_{\alpha\beta}$ contains only real elements.

The scattering matrix of a $2N$-port comprising a set of distinct lengths ℓ_n of lossless transmission line, each with characteristic impedance (resistance) equal to the corresponding port (real) normalization number, is

$$\left(\begin{array}{c|c} 0 & \varepsilon^{-j\Theta} \\ \hline \varepsilon^{-j\Theta} & 0 \end{array}\right), \tag{19a}$$

where Θ is the real diagonal matrix

$$\Theta = \operatorname{diag}\left[\kappa_1 \ell_1, \kappa_2 \ell_2, \ldots, \kappa_N \ell_N\right] . \tag{19b}$$

The corresponding scattering-transfer matrix is therefore

$$\left(\begin{array}{c|c} \varepsilon^{-j\Theta} & 0 \\ \hline 0 & \varepsilon^{j\Theta} \end{array}\right). \tag{20}$$

In general this matrix is not real; hence cascading with its "reverse" does not "undo" the effect of the original network.

Consider the $2N$-port (20) to be terminated by an N-port with scattering matrix S. From (10) one has

$$\left(\begin{array}{c} \mathbf{b}_\alpha \\ \hline \mathbf{b}_\beta \end{array}\right) = \left(\begin{array}{c|c} 0 & \varepsilon^{-j\Theta} \\ \hline \varepsilon^{-j\Theta} & 0 \end{array}\right)\left(\begin{array}{c} \mathbf{a}_\alpha \\ \hline S\mathbf{b}_\beta \end{array}\right), \tag{21}$$

so that

$$\mathbf{b}_\alpha = \left(\varepsilon^{-j\Theta} S \varepsilon^{-j\Theta}\right)\mathbf{a}_\alpha . \tag{22}$$

EIGENWAVE ANALYSIS OF ARRAYS

Uniform Versus General Arrays

For sufficiently large arrays the characteristics of the array (and in particular the eigenvalues) ought to approach those of the infinite array in some sense. Since the eigenvalues for a uniform infinite array of reciprocal antennas are degenerate, we may expect to see degeneracy or near degeneracy in the large finite array. This degeneracy may cause difficulty with some computational algorithms and certainly complicates perturbation analyses.

The uniform circular array shares many of the features of large linear arrays. The eigenvectors for large arrays approach those of the infinite linear array, and the eigenvalues exhibit reciprocity degeneracy (in pairs).

In comparison with uniform arrays of regularly spaced identical antennas, general arrays of nonuniformly spaced antennas have been little used. For this reason, and to dispose of the complicating factor of near degeneracy of the eigenvalue problem to be solved, this report focuses on the uniform case. This is accomplished through symmetry analysis. From the standpoint of computation, then, each of the subspace arrays (odd and even) of a uniform array constitutes a general array in which degeneracies arise only accidentally. The straightforward analysis which is applicable in each subspace therefore also covers the case of the general nonuniform array.

The uniform planar array and the circular cylindrical array generally possess a 180° rotation, reflection, or equivalent symmetry. The eigenvalue problem may be separated in accordance with the invariant subspaces of this symmetry. The formal analysis of this symmetry is taken up next.

Twofold Symmetry Analysis

Consider a uniform linear or uniform circular array with ports numbered as shown in Fig. 5 comprising $N = 2L + 1$ elements. The twofold symmetry operation is represented by the matrix

$$\mathcal{F} = \left(\begin{array}{c|c|c} 0 & 0 & \sigma_L \\ \hline 0 & 1 & 0 \\ \hline \sigma_L & 0 & 0 \end{array}\right) = \mathcal{F}^{-1} \tag{23}$$

operating on a column matrix of terminal quantities ordered as $\mathbf{a}$,

$$\mathbf{a} = \left(\begin{array}{c} \mathbf{a}_\alpha \\ \hline a_0 \\ \hline \mathbf{a}_\beta \end{array}\right), \tag{24a}$$

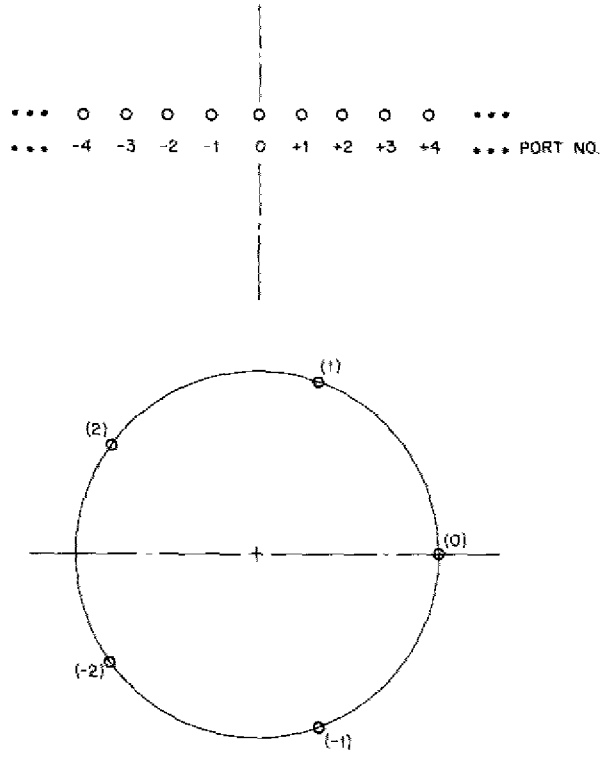

Fig. 5—Uniform linear array and uniform circular array

where

$$\tilde{a}_\alpha = [a_{-L} a_{-L+1} \ldots a_{-2} a_{-1}] \tag{24b}$$

and

$$\tilde{a}_\beta = [a_1 a_2 \ldots a_{L-1} a_L] \,. \tag{24c}$$

The tilde denotes the transpose. The L-dimensional submatrix σ_L is

$$\sigma_L = \begin{pmatrix} 0 & 0 & \ldots & 0 & 1 \\ 0 & 0 & \ldots & 1 & 0 \\ \ldots & \ldots & \ldots & \ldots & \ldots \\ 0 & 1 & \ldots & 0 & 0 \\ 1 & 0 & \ldots & 0 & 0 \end{pmatrix} . \tag{25}$$

The transformation of terminal quantities

$$\mathcal{T}\mathbf{a}' = \mathbf{a}\,, \tag{26}$$

where

$$\mathcal{T} = \frac{1}{\sqrt{2}}\left(\begin{array}{c|c|c} 1_L & 0 & 1_L \\ \hline 0 & \sqrt{2} & 0 \\ \hline \sigma_L & 0 & -\sigma_L \end{array}\right), \tag{27}$$

completely reduces the symmetry operator $\mathcal{F}$ to the form $\mathcal{F}'$:

$$\mathcal{F}' \doteq \mathcal{T}\mathcal{F}\mathcal{T} = \left(\begin{array}{c|c|c} 1_L & 0 & 0 \\ \hline 0 & 1 & 0 \\ \hline 0 & 0 & -1_L \end{array}\right). \tag{28}$$

Note that $\mathcal{T} = \tilde{\mathcal{T}} = \mathcal{T}^{-1}$.

The effect of the transformation $\mathcal{T}$ on the scattering matrix of an array will be illustrated for a circular array with $N = 5$ elements and a linear array with $N = 3$ elements. For the circular array the scattering matrix has the form

$$S = \left(\begin{array}{cc|c|cc} \alpha & \beta & \gamma & \gamma & \beta \\ \beta & \alpha & \beta & \gamma & \gamma \\ \hline \gamma & \beta & \alpha & \beta & \gamma \\ \hline \gamma & \gamma & \beta & \alpha & \beta \\ \beta & \gamma & \gamma & \beta & \alpha \end{array}\right), \tag{29a}$$

where the ports are numbered as shown in Fig. 5 and Eqs. (24). When transformed to primed terminal quantities according to (26),

$$S' = \mathcal{T}S\mathcal{T}$$

$$= \left(\begin{array}{ccc|cc} \alpha+\beta & \alpha+\gamma & \gamma\sqrt{2} & 0 & 0 \\ \beta+\gamma & \alpha+\gamma & \beta\sqrt{2} & 0 & 0 \\ \gamma\sqrt{2} & \beta\sqrt{2} & \alpha & 0 & 0 \\ \hline 0 & 0 & 0 & \alpha-\beta & \beta-\gamma \\ 0 & 0 & 0 & \beta-\gamma & \alpha-\gamma \end{array}\right). \tag{29b}$$

The scattering matrix for a uniform array with $N = 3$ elements has the form

$$S = \begin{pmatrix} \beta & \gamma & \delta \\ \gamma & \alpha & \gamma \\ \delta & \gamma & \beta \end{pmatrix}, \tag{30a}$$

where again the ports are numbered as shown in Fig. 5 and Eqs. (24). When transformed to primed terminal quantities according to (26),

$$S' = \mathfrak{T} S \mathfrak{T} = \left(\begin{array}{cc|c} \beta + \delta & \gamma\sqrt{2} & 0 \\ \gamma\sqrt{2} & \alpha & 0 \\ \hline 0 & 0 & \beta - \delta \end{array}\right). \tag{30b}$$

Consider now the conventional set of eigenvectors for a circular array

$$\mathbf{t}^{(m)} = \left[t_\ell^{(m)} \right], \quad -L \leqslant \ell \leqslant L, \tag{31a}$$

and

$$t_\ell^{(m)} = \frac{1}{\sqrt{N}} \exp j \left(\frac{2\pi}{N} m\ell \right). \tag{31b}$$

These also constitute the conventional form of excitation for the linear phased array, although they are eigenvectors of such an array, only for the case $\ell, m \to \infty$. The latter can be deduced from considerations of symmetry. The complex-conjugate eigenvectors are degenerate; that is, the eigenvalues belonging to distinct complex eigenvectors (m) and $(-m)$ are the same. The same pairing is accomplished by the operator $\mathfrak{T}$. $\mathfrak{T}$ also effects a change of sign in the exponent in Eq. (31) through a change in the sign of ℓ. It follows that

$$\mathbf{u}^{(n)} = \frac{1}{2}(1 \pm \mathfrak{T})\mathbf{t}^{(m)}, \quad -L < m < L, \tag{32}$$

is also an eigenvector (possibly the same eigenvector) of the circular or infinite linear array. Therefore these new eigenvectors of the array are by construction (a) real and (b) eigenvectors of $\mathfrak{T}$. A different labeling n is usually convenient for the vectors $\mathbf{u}^{(n)}$. The correspondence of n and m is in any event established by (32).

The eigenvectors of $\mathfrak{T}$ are classed as either even (belonging to the eigenvalue +1) or odd (belonging to the eigenvalue −1): the vector

$$\mathbf{u}^{(n)} = \frac{1}{2}(1 + \mathfrak{T})\mathbf{t}^{(m)} \tag{33a}$$

is even, and the vector

$$\mathbf{u}^{(n)} = \frac{1}{2}(1 - \mathcal{F})\mathbf{t}^{(m)} \tag{33b}$$

is odd.

The operators $(1/2)(1 \pm \mathcal{F})$ of Eqs. (33) are readily shown to be projection operators associated with orthogonal subspaces whose direct sum is the complete space. They are projection operations (idempotent):

$$\left[\frac{1}{2}(1 \pm \mathcal{F})\right]^2 = \frac{1}{2}(1 \pm \mathcal{F}) . \tag{34a}$$

They are orthogonal:

$$\frac{1}{2}(1 + \mathcal{F})\,\frac{1}{2}(1 - \mathcal{F}) = \frac{1}{2}(1 - \mathcal{F})\,\frac{1}{2}(1 + \mathcal{F}) = 0 . \tag{34b}$$

And they are complete:

$$\frac{1}{2}(1 + \mathcal{F}) + \frac{1}{2}(1 - \mathcal{F}) = 1 . \tag{34c}$$

To make these results concrete, the form of the matrix transformation which sorts out the eigenvectors according to the above scheme is computed explicitly. Recall that $\mathcal{T} = \mathcal{T}^{-1}$ and that

$$\mathcal{T}\mathbf{u}'^{(n)} = \mathbf{u}^{(n)} ; \tag{35a}$$

therefore

$$\mathbf{u}'^{(n)} = \frac{1}{2}\mathcal{T}(1 \pm \mathcal{F})\mathbf{t}^{(m)} . \tag{35b}$$

The transformation $\mathcal{T}$ sorts any even portion of $\mathbf{u}^{(n)}$ into the first $L + 1$ rows of the vector $\mathbf{u}'^{(n)}$ and any odd portion of $\mathbf{u}^{(n)}$ into the last L rows of $\mathbf{u}'^{(n)}$. When the matrix product in (35b) is computed using the explicit representations of $\mathcal{F}$ (Eq. (23)), and $\mathcal{T}$ (Eq. (27)), one finds

$$\frac{1}{2}\mathcal{T}(1 + \mathcal{F}) = \frac{1}{\sqrt{2}}\left(\begin{array}{c|c|c} 1_L & 0 & \sigma_L \\ \hline 0 & \sqrt{2} & 0 \\ \hline 0 & 0 & 0 \end{array}\right) \tag{36a}$$

and

$$\frac{1}{2}\mathcal{T}(1 - \mathcal{F}) = \frac{1}{\sqrt{2}}\left(\begin{array}{c|c|c} 0 & 0 & 0 \\ \hline 0 & 0 & 0 \\ \hline 1_L & 0 & -\sigma_L \end{array}\right) . \tag{36b}$$

From the placement of zeros in (36a) and (36b) it is clear that $(1 + \mathfrak{F})$ has projected out the even part of $\mathbf{t}^{(m)}$, so that the last L rows of $\mathbf{u}'^{(n)}$ are necessarily zeros, and that $(1 - \mathfrak{F})$ has projected out only the odd part of $\mathbf{t}^{(m)}$, so that the first $L + 1$ rows of $\mathbf{u}'^{(m)}$ are necessarily zeros.

In summary the preceding analysis shows that the degenerate eigenvalues of the circular and infinite linear array are split between the two invariant subspaces belonging to $\mathfrak{F}$ and that the two separate reduced subspaces will contain only accidental degeneracies. The eigenvectors $\mathbf{u}'^{(n)}$, properly renormalized where necessary, may be employed together with straightforward nondegenerate perturbation theory to solve for the eigenvectors of finite linear arrays.

CALCULATION OF ELEMENT PATTERNS FOR SUITABLY MATCHED ARRAYS

Excitation and the Radiation Fields

An elementary radiator of an array is usually specified in terms of its properties when isolated from the array environment. In a dipole array, for example, the elementary dipole is commonly specified in terms of the properties of the isolated dipole. This information is in general not sufficient to permit calculation of an element pattern in the array environment. However, when all antennas but the one antenna element excited are terminated in some fixed reactance, the element pattern in the array environment may be nearly the same as the isolated antenna pattern. An array of small dipoles is one example. When all dipoles but one are open-circuited, the pattern of the single dipole is nearly that of an isolated dipole. An array of slots in a large ground plane is another. When all slots but one are short-circuited, the pattern of the single excited slot is nearly that of a single slot in a ground plane. For canonical minimum-scattering antennas [11] the element patterns in the open-circuited array environment coincide with the isolated-element patterns. Without any restrictions on antenna type it will be assumed in this section that the radiated field of a single excited element in the open-circuited-array environment is a known complex vector function of the direction angles θ and ϕ

$$\vec{f}^{(o)}(\theta, \phi) \tag{37}$$

and is normalized so that with unit incident power excitation the radiated power is

$$P_{\text{rad}} = \int |\vec{f}^{(o)}(\theta, \phi)|^2 \, d\Omega$$

$$= 1 - \left|\frac{Z_0 - Z_g^*}{Z_0 + Z_g}\right|^2 , \tag{38}$$

where Z_0 is the input impedance to the excited element and $d\Omega$ is the element of solid angle $\sin\theta \, d\theta d\phi$. A common alternative normalization fixes on the radiation amplitude produced by a unit input current; this field will be distinguished by an I subscript, $\vec{f}_I(\theta, \phi)$. The corresponding power normalization is then

$$P_{\text{rad}} = \int |\vec{f}_I^{(o)}(\theta, \phi)|^2 \, d\Omega = \text{Re}\, Z_0 \,. \tag{39}$$

Since for this open-circuit-environment condition

$$\begin{aligned} 2\sqrt{R_g}\, a &= V + Z_g I \\ &= (Z_0 + Z_g) I \,, \end{aligned} \tag{40}$$

it follows that

$$\vec{f}_I^{(o)}(\theta, \phi) = \frac{Z_0 + Z_g}{2\sqrt{R_g}} \vec{f}^{(o)}(\theta, \phi) \,. \tag{41}$$

In the special case $Z_0 = Z_g^*$

$$\vec{f}_I^{(o)}(\theta, \phi) = \sqrt{R_g}\, \vec{f}^{(o)}(\theta, \phi) \,. \tag{42}$$

Since $\vec{f}_{I,n}^{(o)}(\theta, \phi) I_n$ is the pattern radiated by the nth element when all the remaining currents are zero (open-circuit condition), one may employ straightforward superposition to obtain the field for any set of currents. In particular, if the *correct* I_n corresponding to matched terminations at each element have been found from the mutual coupling constraints ($\mathbf{V} = Z\mathbf{I}$ or $\mathbf{b} = S\mathbf{a}$), then the field radiated by some element in the terminated array environment for that element is

$$\begin{aligned} \vec{f}(\theta, \phi) &= \sum_{n=-L}^{L} \vec{f}_{I,n}^{(o)}(\theta, \phi) I_n \\ &= \frac{Z_{0n} + Z_g}{2\sqrt{R_g}} \sum_{n=-L}^{L} \vec{f}_n^{(o)}(\theta, \phi) I_n \,. \end{aligned} \tag{43}$$

In the terminated-array environment the correct currents produced by a real generator are most easily expressed in terms of scattering quantities

$$\begin{aligned} \sqrt{R_g} I_n &= a_n - b_n \\ &= \sum_{m=-L}^{L} (\delta_{nm} - S_{nm}) a_m \\ &= a_n' \,. \end{aligned} \tag{44}$$

Note the difference between the open-circuit conditions (40) and the terminated-port condition expressed by (44). Using (44),

$$\vec{f}(\theta, \phi) = \frac{Z_{0n} + Z_g}{2R_g} \sum_{n=-L}^{L} \vec{f}^{(o)}(\theta, \phi) a'_n . \tag{45}$$

The Modified Array

The input impedance matrix for an array of antennas, considered as a dissipative N-port, generally has both resistive components R_{mn} and reactive components X_{mn}:

$$Y_n = \sum_{n=1}^{N} Z_{mn} I_n , \tag{46}$$

where

$$Z_{mn} = R_{mn} + jX_{mn} .$$

The resistive components are directly related to the element patterns in the open-circuited environment through the conservation of energy:

$$R_{mn} = \mathrm{Re} \int \vec{f}^{(o)}_{l,m}(\theta, \phi) \cdot \vec{f}^{(o)*}_{l,n}(\theta, \phi)\, d\Omega . \tag{47}$$

The imaginary components have no such unique relationship with the patterns, although in special cases the imaginary components may be connected with the analytic continuation of the real patterns into the complex angular domain [11]. These reactive components may obviously be canceled through a lossless reactance network, one form of which is shown as

$$jB = j[B_{mn}] = +j[-R_t^{-2} X_{mn}]$$

in Fig. 6 and is described in more detail subsequently. The combination of the array plus this cancellation network is termed the *modified array*. The modified array has the real input impedance matrix $R = [R_{mn}]$.

The lossless reactance cancellation network in Fig. 6 is formed by attachment of quarter wavelengths of transmission line at each antenna port. If the transmission lines all have the same characteristic impedance R_t, then the input short-circuit *admittance* matrix of the array plus transmission lines is

$$Y = R_t^{-2} Z = [R_t^{-2} Z_{mn}] . \tag{48}$$

At this point then the shunt susceptance network $jB = -j\ \mathrm{Im}\ Y$ is connected to produce the desired cancellation effect. The addition of a second set of quarter-wavelength transmission lines, also of characteristic impedance R_t, reconverts the residual real part of the admittance matrix, Re Y, into the impedance matrix $R = [R_{mn}] = R_t^2\ \mathrm{Re}\ Y$.

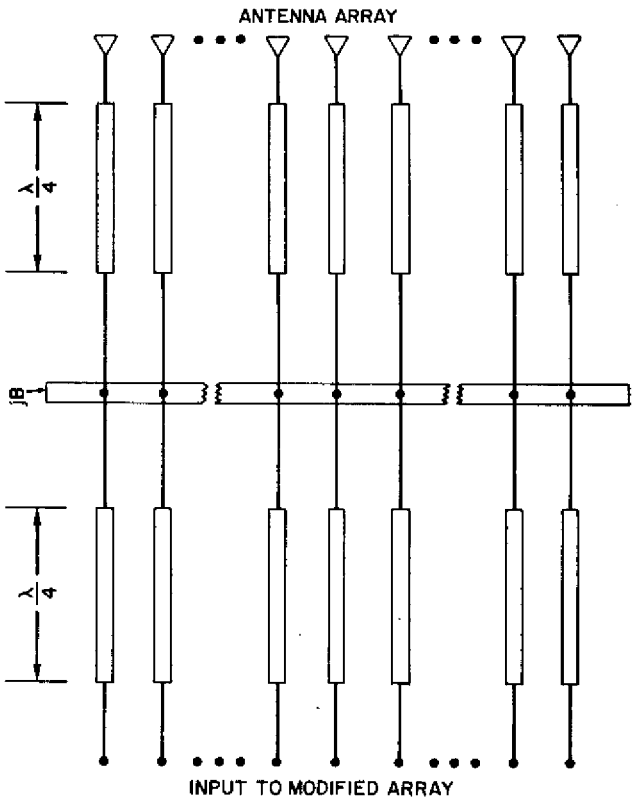

Fig. 6—Modified array

Matching Network for the Modified Linear Array

The general scheme of the matching network which will be employed in our calculations is shown in Fig. 7. There are three main sections: the first section (drawn as three large rectangles) is a real transparent $2N$-port, the second section (drawn as N small rectangles) consists of N disjoint lossless two-ports, and the third section (drawn as three large rectangles—a mirror image of the first section) is a real transparent $2N$-port—the "reverse" of the first section. If the two-ports of the second section were just direct connections, the first and third sections would "undo" one another. Excitation supplied at the left then would appear at the *correspondingly labeled* antenna input port at the right. This apparently trivial point of notation is essential to preserve the physical significance of our results. We now specify each of these sections in more detail.

The large rectangle of the first section of Fig. 7 separates all array excitations into even and odd portions as discussed earlier. The scattering matrix of this $2N$-port [12] is

$$S_{\mathcal{T}} = \left(\begin{array}{c|c} 0 & \mathcal{T} \\ \hline \tilde{\mathcal{T}} & 0 \end{array}\right), \tag{49}$$

where $\mathcal{T}$, the transformation (26), is such that

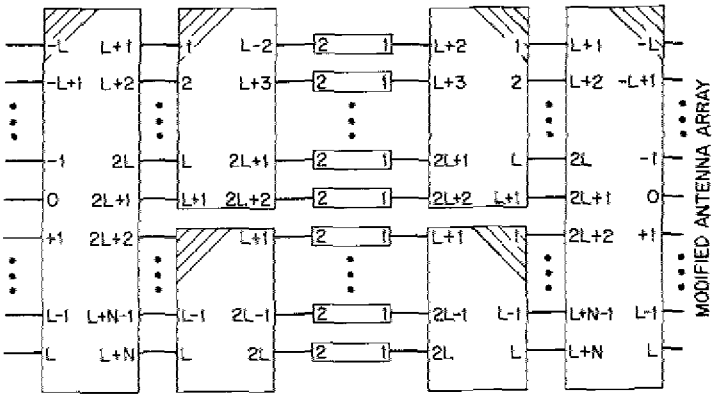

Fig. 7—Matching network for symmetric array

$$S' = \tilde{\mathcal{T}} S \mathcal{T} = \left(\begin{array}{c|c} S_{(+)} & 0 \\ \hline 0 & S_{(-)} \end{array}\right). \tag{50}$$

The matrices $S_{(+)}$ and $S_{(-)}$ are the even and odd submatrices of the antenna-array scattering matrix S.

The two smaller rectangles of the first section have the $2(L+1)$-by-$2(L+1)$ scattering matrix

$$S_{\mathcal{T}(+)} = \left(\begin{array}{c|c} 0 & \mathcal{T}_{(+)} \\ \hline \tilde{\mathcal{T}}_{(+)} & 0 \end{array}\right) \tag{51a}$$

and the $2L$-by-$2L$ scattering matrix

$$S_{\mathcal{T}(-)} = \left(\begin{array}{c|c} 0 & \mathcal{T}_{(-)} \\ \hline \tilde{\mathcal{T}}_{(-)} & 0 \end{array}\right) \tag{51b}$$

respectively, where $\mathcal{T}_{(+)}$ and $\mathcal{T}_{(-)}$ are matrices whose columns are the real, normalized eigenvectors of the even and odd subscattering matrices $S_{(+)}$ and $S_{(-)}$ in some arbitrary (but thereafter fixed) order. For a detailed description of the third section of the matching network, it now suffices to state it is the "reverse" of the first section.

The second or middle section performs the matching function. A typical 2-port section is shown in Fig. 8. The scattering matrix of this transformer matching section is

$$\begin{pmatrix} +\rho & \sqrt{1-\rho^2} \\ \sqrt{1-\rho^2} & -\rho \end{pmatrix}, \tag{52}$$

where

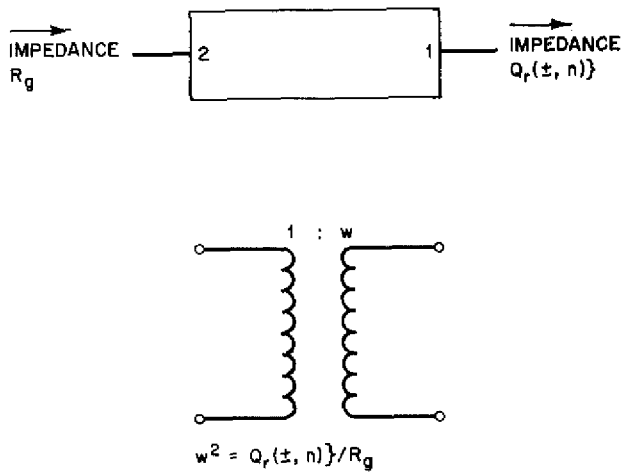

Fig. 8—Typical transformer matching 2-port

$$\rho = \rho(\pm, n) = \frac{Q_r(\pm, n) - R_g}{Q_r(\pm, n) + R_g}. \tag{53}$$

The notation $Q_r(\pm, n)$ refers to the input impedance at the nth even (+) or nth odd (−) matching two-port, which is connected between the two nth output ports of the networks $S_{(\pm)}$ and its reverse. $Q_r(\pm, n)$ is, by construction, the nth even or nth odd eigenvalue of the modified antenna array resistance matrix R.

For an incident wave a_2 at terminal 2 of a matching 2-port, a wave amplitude b_1 is generated at terminal 1 in accordance with (52):

$$b_1 = \rho a_1 + \sqrt{1 - \rho^2}\ a_2. \tag{54a}$$

As arranged, $b_1 = 0$, which means that

$$0 = \sqrt{1 - \rho^2}\ a_1 - \rho a_2; \tag{54b}$$

hence

$$b_1 = \left(\frac{\rho^2}{\sqrt{1 - \rho^2}} + \sqrt{1 - \rho^2}\right) a_2$$

$$= \frac{a_2}{\sqrt{1 - \rho^2}}. \tag{54c}$$

This is the wave which is *incident on* the first-section port and results in an incident wave on the modified array of $\mathbf{e}(1 - \rho^2)^{-1/2} a_2$, where $\mathbf{e}$ is the eigenvector of R corresponding to the port excited by a_2. At the ports of the modified array a reflected wave, ρ times

the incident wave, is generated. The currents (44) at the modified array, proportional to the difference of incident and reflected amplitudes, are elements of the column matrix

$$R_g^{-1/2}(1-\rho)\mathbf{e}(1-\rho^2)^{-1/2}a_2 . \tag{55}$$

The eigenvectors of the scattering matrix of the modified array S can be calculated from the eigenvectors of $S_{(\pm)}$. If the matrix eigenvectors of $S_{(+)}$ is $\mathcal{E}_{(+)}$ and of $S_{(-)}$ is $\mathcal{E}_{(-)}$, that is,

$$\mathcal{E}_{(+)} = [\mathbf{e}(+,1)\mathbf{e}(+,2) \ldots \mathbf{e}(+,L+1)] \tag{56a}$$

$$\mathcal{E}_{(-)} = [\mathbf{e}(-,1)\mathbf{e}(-,2) \ldots \mathbf{e}(-,L)] , \tag{56b}$$

then

$$\begin{aligned} \mathcal{E} &= [\mathbf{e}(-L)\mathbf{e}(-L+1) \ldots \mathbf{e}(0) \ldots \mathbf{e}(L)] \\ &= \mathcal{T}\left(\begin{array}{c|c} \mathcal{E}_{(+)} & 0 \\ \hline 0 & \mathcal{E}_{(-)} \end{array}\right)\tilde{\mathcal{T}} . \end{aligned} \tag{57}$$

With these definitions, for arbitrary input $\mathbf{a}$ to the matching network, Fig. 7, the currents at the inputs to the modified array are

$$\sqrt{R_g}\,\hat{\mathbf{i}} = \hat{\mathbf{a}} - \hat{\mathbf{b}} \tag{58a}$$

$$\begin{aligned} &= \mathcal{E}(1-\rho)(1-\rho^2)^{-1/2}\tilde{\mathcal{E}}\mathbf{a} \\ &= \mathcal{E}[(1-\rho)(1+\rho)^{-1}]^{1/2}\tilde{\mathcal{E}}\mathbf{a} \\ &= \mathcal{E}[Q_r]^{-1/2}\tilde{\mathcal{E}}\mathbf{a} , \end{aligned} \tag{58b}$$

where ρ is now the diagonal matrix

$$\rho = \operatorname{diag}[\rho(-L), \ldots, \rho(0), \ldots, \rho(L)] \tag{59a}$$

and the matrix Q_r is given by

$$Q_r = \operatorname{diag}[Q_r(-L), \ldots, Q_r(0), \ldots, Q_r(L)] . \tag{59b}$$

From the definition of $\mathcal{E}$, (58b) may be rewritten

$$\sqrt{R_g}\,\hat{\mathbf{i}} = R^{-1/2}\mathbf{a} \tag{60}$$

as anticipated.

Partial Match of the Array

Although an array can be matched for almost all excitations by means of the feed network developed in the preceding paragraphs, an exceptional circumstance occurs when one of the eigenvalues of the resistance matrix is zero or infinite. This can happen with an array of lossless antenna elements which actually fail to radiate and therefore present a purely reactive impedance, which case is excluded from further consideration because of its triviality. Even with an array of bona-fide antennas (antennas which are not purely reactive) this exceptional circumstance can occur "accidentally." By this is meant an occurrence which can be removed simply by an infinitesimal perturbation of the array. Again, this is of little interest here. However for large closely-spaced regular arrays a set of small (or large) eigenvalues occurs in a nonaccidental fashion which consequently is of physical interest.

As has already been mentioned, the characteristics of a large finite array approach those of the infinite array. In the infinite-array model eigenexcitations produce either delta-function beams (visible region) or no beams at all (invisible region) [13]. The active impedance (eigenvalue) corresponding to an excitation which does not place a beam in visible space is purely reactive. The large finite array with the same spacing does not preserve this absolute distinction between visible and invisible regions, because the patterns of any finite array are not indefinitely narrow. Some energy is directed along almost all real angles. An excitation which would produce in-phase addition only at complex angles (in the invisible region) in the case of finite arrays radiates into visible space through a sidelobe. However the active input resistance corresponding to this condition is much smaller or larger than unity or R_g. Attempts to realize match in these cases are subject to limitations closely akin to those associated with the realization of supergain [9]. This aspect of the match problem will be illustrated later.

The matching network, Figs. 7 and 8, leaves the corresponding eigenexcitation unaffected when the turns ratio of the transformer two-port (Fig. 8) corresponding to that particular eigenexcitation is replaced by a straight connection or equivalently the turns ratio is set equal to unity: $w = 1$. A wave a_1 incident at the input to this transformer produces wave amplitudes $\mathbf{e}a_1$ incident on the modified array, $\mathbf{e}$ being the eigenvector of S involved. The corresponding currents exciting the modified array (44) are then $R_g^{-1/2}\mathbf{e}(1-\rho)a_1$. In general therefore (58) must be replaced by

$$\sqrt{R_g}\,\mathbf{I} = \mathbf{a} - \mathbf{b} \tag{61a}$$

$$= \mathcal{E}\mathcal{P}\tilde{\mathcal{E}}\mathbf{a}\,, \tag{61b}$$

where

$$\mathcal{P} = \operatorname{diag}\left[\ldots, \left(\frac{1-\rho(m)}{1+\rho(m)}\right)^{1/2}, \ldots, (1-\rho(n)), \ldots\right] \tag{62a}$$

$$= \operatorname{diag}\left[\ldots, Q_r^{-1/2}(m), \ldots, \frac{2R_{gn}}{Q_r(n)+R_{gn}}, \ldots\right]. \tag{62b}$$

In Eqs. (62) it is understood that the first expression within the brackets applies to eigen-excitations (eigenvalues) that are matched and the second applies to eigenvalues that are not matched. The currents (61) are now no longer simply related to $R^{1/2}$ and cannot be found simply from energy considerations.

APPLICATION AND EXAMPLES

The preceding theory will now be applied to a linear array of infinite line sources. The theory is in no way limited to uniform arrays, nor are the computations appreciably simplified by the assumption of uniformity. Uniform arrays are chosen because of their practical importance and because the comparison of the finite-array results with those obtained for the corresponding infinite array [4] is of special interest. Pertinent results obtained in Ref. 4 are summarized in Appendix A for convenience.

Consider an array of line sources distributed along the x axis of a Cartesian coordinate system, each line source being of infinite extent and parallel to the z axis. The pattern of an individual line-source element is isotropic in the xy plane. The line source may be one of electric current (in which case the electric vector is polarized along the z axis), or the line source may be one of magnetic current, simulating a narrow slot in a conducting plane (in which case the magnetic vector is polarized along the z axis). The mutual coupling between such elements may be computed on the assumption of a single-mode element [14] or a canonical minimum-scattering antenna [11]. The result for either polarization is (at appropriate reference planes) [11]

$$\begin{aligned} Z_{mn} &= 1\,, \quad m = n\,, \\ &= H_0^{(2)}(k\,|x_m - x_n|)\,, \quad m \neq n\,, \end{aligned} \tag{63}$$

where x_n is the coordinate at which the line source intercepts the x axis, $H_0^{(2)}$ is the Hankel function of the second kind and zeroth order, and k is the wave number $2\pi/\lambda$. The impedance matrix of the "modified array" comprises the real elements

$$\begin{aligned} R_{mn} &= 1\,, \quad m = n\,, \\ &= J_0(k\,|x_m - x_n|)\,, \quad m \neq n\,, \end{aligned} \tag{64}$$

where J_0 denotes the Bessel function of the first kind and zeroth order.

Figure 9 shows element patterns in the terminated-array environment for the center elements of uniform arrays as dotted lines. The elements of the array are $kD = \pi$ radians apart, and the arrays consist respectively, of 5, 15, and 25 elements. In each case the center element is excited by an incident wave carrying unit power. In comparing the results obtained with those for the infinite array (Appendix A) it must be remembered that the infinite-array formulas are conventionally quoted for radiation into a halfspace. Account of this is taken if the directly computed absolute power patterns are multiplied by a factor of 2. For uniformity of presentation both the finite-array patterns and the infinite-array pattern were further divided by kD/π. This has the effect of normalizing the element patterns for any spacing. The normalized infinite-array element pattern is

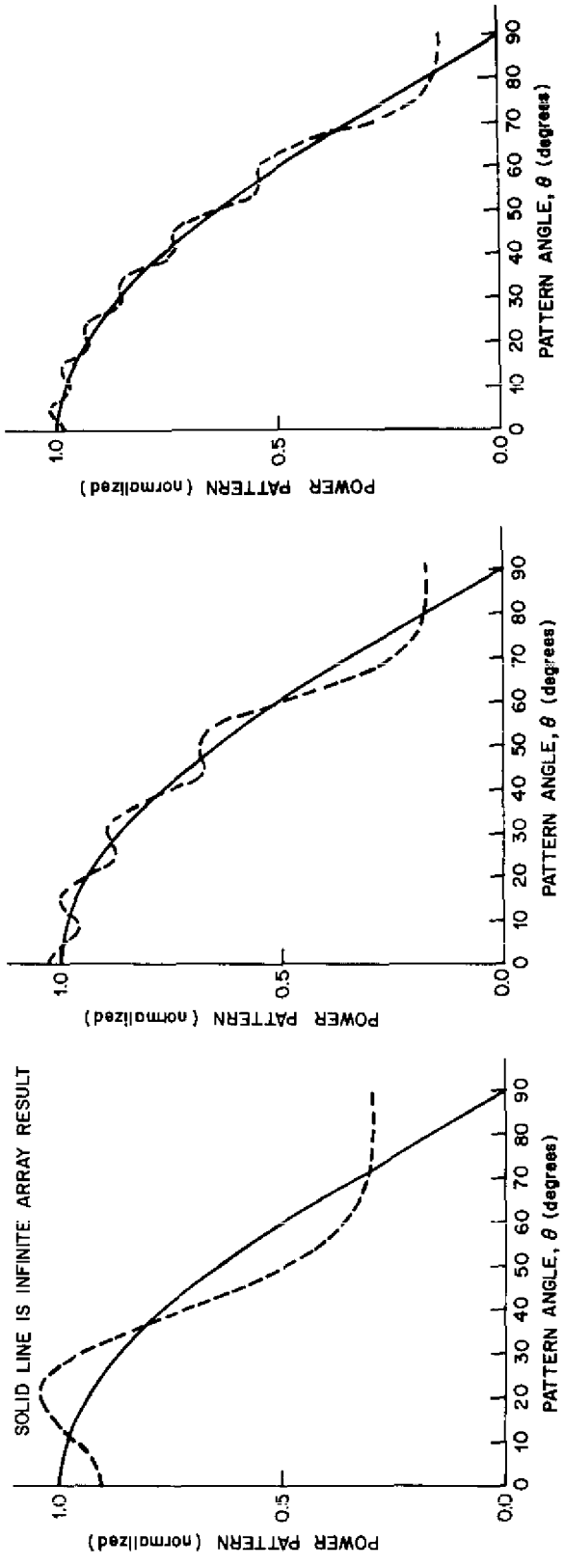

(a) $N = 5$ elements (b) $N = 15$ elements (c) $N = 25$ elements

Fig. 9—Element patterns for the center elements of linear arrays of line sources with elements spaced $kD = \pi$ radians apart. The solid line is the infinite-array result.

shown as a solid line. It is clear that the element pattern for a matched array approaches the infinite-array result. The approach is oscillatory (after the fashion of trigonometric series) rather than smooth. For $N = 25$ elements the pattern closely follows the infinite-array result except in the immediate neighborhood of radiation along the plane of the array, $\theta = 90°$. This result is in agreement with the expectations based on element efficiency [5].

Only half of each element pattern is shown in each case, because the power patterns are symmetric with respect to $\theta = 0$. In the case of linear or planar arrays, this symmetry is always a feature of (optimally) matched element patterns, since the currents exciting each element of the radiating aperture are real (either in phase or 180° out of phase.) That these currents are indeed real is evident from (60) or (61), for $\mathbf{a} = [\delta_{n\ell}]$, that is, when only the ℓth input to the feed network is excited by a unit incident wave.

The element pattern in the terminated-array environment for an edge element of the $N = 25$ array is shown in Fig. 10. Its shape is somewhat broadened when referred to a $\cos\theta$ pattern and the peak gain is reduced approximately 0.7 dB.

Element patterns in the terminated-array environment for an array of $N = 25$ elements spaced $kD = 4.0$ radians apart are shown in Fig. 11. The element pattern for the center element is shown in Fig. 11a, and the edge effect present at this spacing is displayed in Figs. 11b, 11c, and 11d. The center-element pattern in Fig. 11a displays a close oscillatory approach to the infinite-array element pattern. The sharp break to a null at 34.8° in the infinite-array element pattern associated with the entry of a grating lobe is evident also in the finite-array patterns. Of course the finite-array element patterns do not have an absolute null. As before, the largest deviations occur in the neighborhood of the array face ($\theta = 90°$). The peak gain of the edge element (Fig. 11b) is reduced by approximately 0.8 dB. In the second and third element from the edge of the array (Figs. 11c and 11d) the sharpness of the features associated with entry of the grating lobe appear

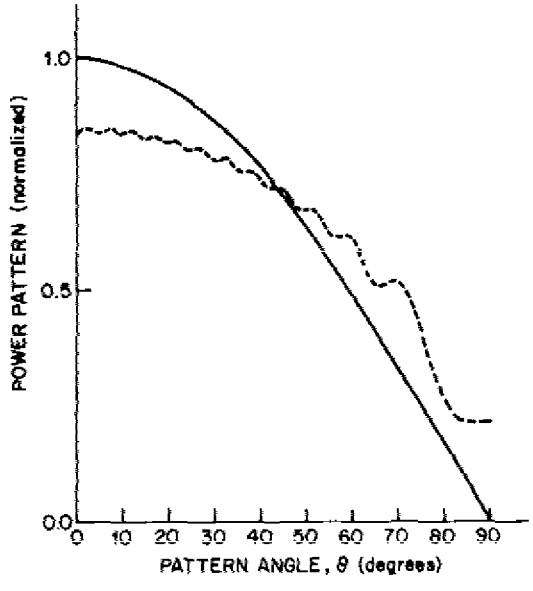

Fig. 10—Element pattern for the edge element ($\ell = 12$) of a linear array of line sources with $N = 25$ elements spaced $kD = \pi$ radians apart

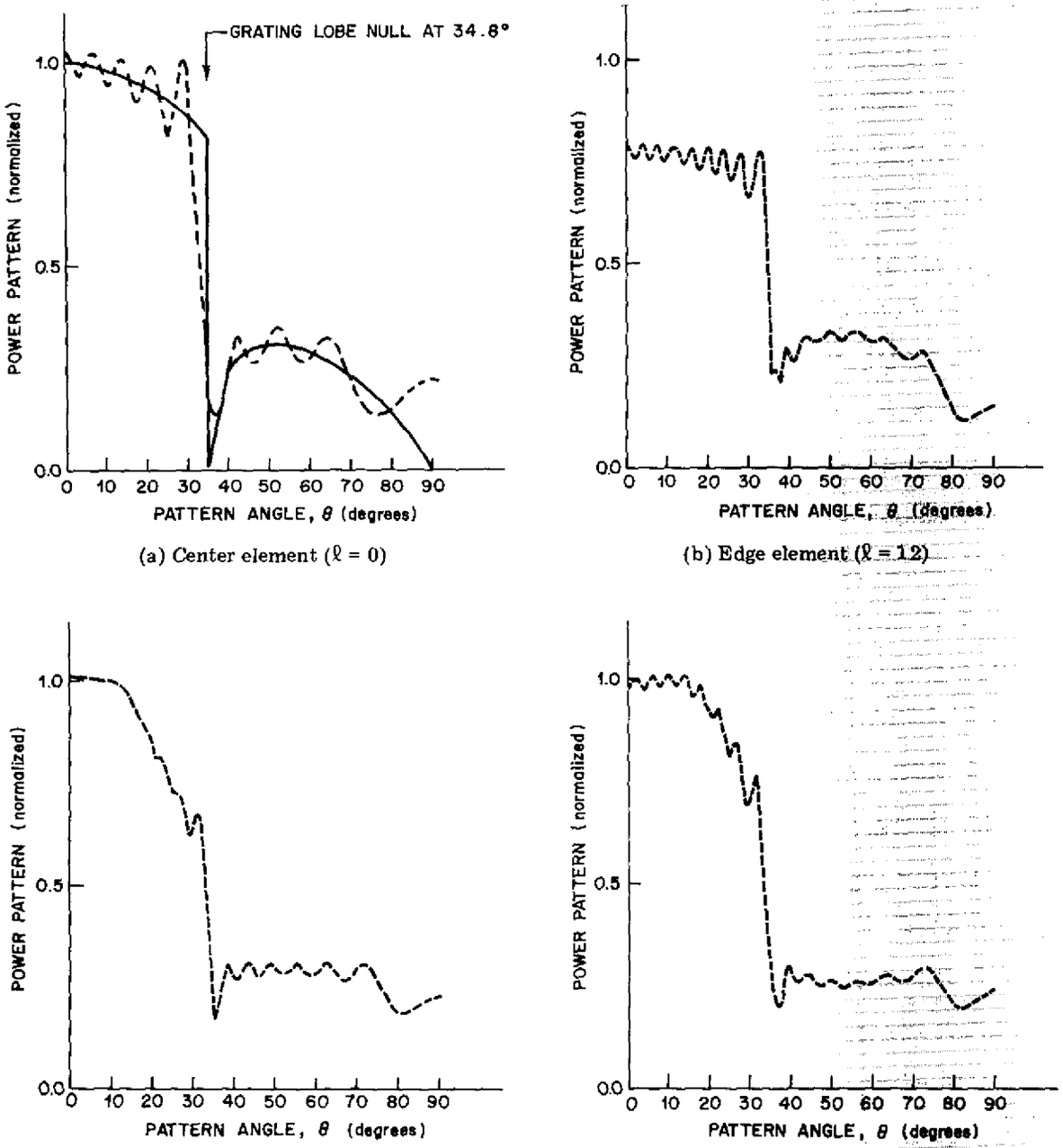

(a) Center element ($\ell = 0$)

(b) Edge element ($\ell = 12$)

(c) Second element from the edge ($\ell = 11$)

(d) Third element from the edge ($\ell = 10$)

Fig. 11—Element patterns for various elements of a linear array of line sources with $N = 25$ elements spaced $kD = 4.0$ radians apart

somewhat smoothed. The overall effect of this smoothing is to narrow the main lobe of the element pattern.

In the preceding examples it was feasible to match the arrays for all excitations; that is, Eq. (60) could be employed to compute the currents exciting the modified array. For spacings $kD < \pi$ we must be prepared to implement an appropriate partial match.

Consider now a closely spaced array of line sources, with elements spaced $kD = 2.0$ radians apart. The eigenvalues of the mutual-resistance matrix for the modified array are listed in Table 1. It is clear that some of these eigenvalues imply active reflection coefficients differing in magnitude only slightly from unity. This is in accordance with our expectations based on the infinite-array model. In an infinite array with this close spacing there is a continuum of (eigen) excitations for which the active reflection coefficient necessarily has unit magnitude.

Figure 12a shows the element pattern in the terminated array environment for the center element of the array when the array is matched for all those eigenexcitations for which the eigenreflection-coefficient magnitude is $|\rho(n)| < 0.5$. The corresponding range of eigenvalues of the mutual-resistance matrix is $0.33 < Q_r(n) < 3.0$. The remaining eigenexcitations of the modified array are left undisturbed. The eigenvalues which were left unmatched are italicized in Table 1. Consequently 15 of the 25 eigenexcitations were matched to achieve the pattern shown in Fig. 12a. Note that 15 is nearly the number of half wavelengths in the aperture: $NkD/\pi = 15.91$. The fraction of elements which may readily be matched is approximately equal to the ideal element efficiency of the corresponding infinite array, $\eta = kD/\pi$ [5,9].

Figures 12b and 12c show the same element pattern when tolerances on the eigenvalues of the resistance matrix $Q_r(n)$ are respectively $0.05 < Q_r(n) < 20$ and $0.001 < Q_r(n) < 1000$. These tolerances correspond to ignoring eigenreflection-coefficient magnitudes $|\rho(n)| \geqslant 0.9$ and $|\rho(n)| \geqslant 0.998$. When *all* eigenvalues are matched, a pattern with wide oscillations results (Fig. 12d). As total match for all excitations is approached, the pattern oscillations widen, and a large lobe spills over into visible space near 90°.

Thus the difficulties associated with matching extreme values of the active resistance $Q_r(n)$ are akin to those involved in the attainment of supergain. Supergain is evidenced

Table 1—The 25 Eigenvalues $Q_r(n)$ of the Mutual-Resistance Matrix for a Linear Array of Line Sources With $N = 25$ Elements Spaced $kD = 2.0$ Radians Apart (The eigenvalues in italics are outside the range $0.33 < Q_r(n) < 3.0$)

3.28225	1.41119	1.07501	1.00214	6.23879×10^{-5}
3.18452	1.26061	1.05742	0.862315	2.23549×10^{-6}
1.85831	1.22749	1.03141	1.83745×10^{-1}	5.43821×10^{-8}
1.79140	1.14601	1.01972	1.83886×10^{-2}	3.88444×10^{-9}
1.45741	1.12175	1.00759	1.25242×10^{-3}	1.94222×10^{-9}

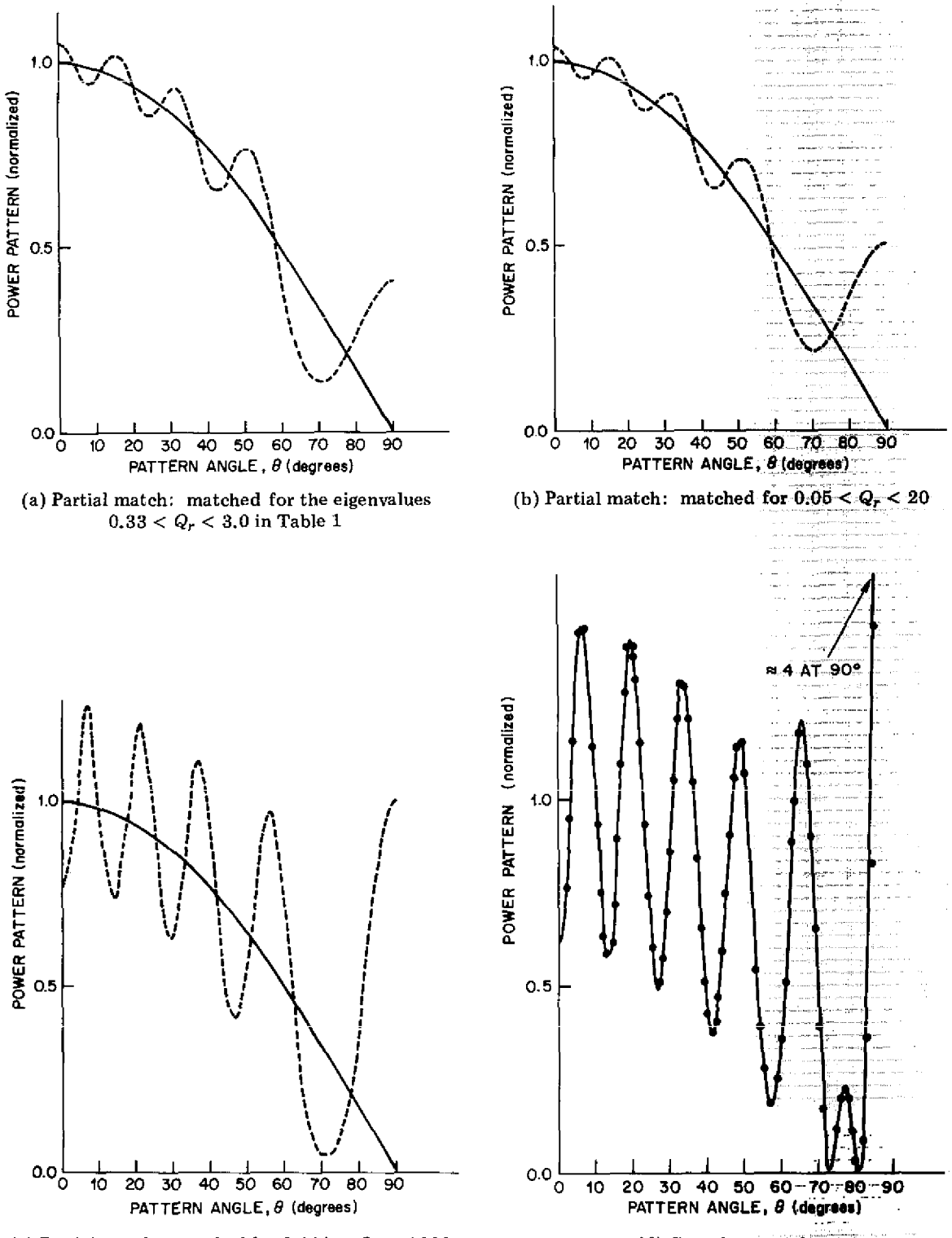

(a) Partial match: matched for the eigenvalues $0.33 < Q_r < 3.0$ in Table 1

(b) Partial match: matched for $0.05 < Q_r < 20$

(c) Partial match: matched for $0.001 < Q_r < 1000$

(d) Complete match

Fig. 12 — Element patterns for the center element of a linear array of line sources with $N = 25$ elements spaced $kD = 2.0$ radians apart

even in the element patterns. The power pattern for an element of the infinite array, as computed from Hannan's formula, attributes to each element the normal gain $kD \cos \theta$ associated with the area per array element [2]. (For the linear array $2\pi D/\lambda$ replaces the planar-array expression $4\pi A/\lambda^2$.) Thus power radiated in excess of the power per radian predicted by Hannan's formula (the solid line in Fig. 12) represents the degree of supergain attained. This excess is slight as long as the active impedance mismatch (eigenreflection coefficients) tuned out are modest.

DISCUSSION AND CONCLUSIONS

The wider implications of the results presented in this report lie in confirmation that constraints on array performance predicted by the relatively simple infinite-array model effectively operate as constraints on the performance of finite arrays in a manner and to an extent illustrated by the detailed calculations presented. These constraints limit the attainable element patterns, including specific features of these such as grating-lobe nulls, and limit the attainable reduction of mutual coupling among antennas by appropriate feed network design. Confirmation of the effectiveness of these constraints in finite arrays is required, since the reasoning employed to establish them in the case of the infinate array cannot be carried over to the finite case. Indeed the general physical grounds for the constraints disappear in the finite array. These physical grounds are replaced by more complex and special mutual-coupling effects. Consequently the phrase "effectiveness of the constraints" is used.

Reasoning based on the conservation of energy and symmetry shows that the pattern of a single element excited by a unit incident wave in the environment of an infinite regular planar array of identical terminated elements must satisfy [2,3]

$$P(\theta) \leqslant \frac{D_x}{\lambda} \cos \theta \ . \tag{65}$$

In particular equality can hold only in the matched case, when the active reflection coefficient (for all elements excited with uniform amplitude and linear phase) is zero. The form of the element pattern for a matched infinite array is given explicitly by Eq. (A1) of Appendix A. The generality of the physical grounds is such that (65) applies independent of the type of antenna elements employed. This limitation is particularly severe at wide angles ($\theta \approx \pi/2$) in that it entirely precludes radiation parallel to the plane of the array. The finite arrays of line sources used as examples constitute a particularly rigorous test of this prediction from the infinite-array model, since individually the line-source elements radiate isotropically in the plane normal to the line source.

Figure 9 shows the extent to which this infinite-array constraint remains effective. As is also possible in the case of an infinite array with spacing $kD_x = \pi$, where $D_x = \lambda/2$, each finite array is matched for *all* excitations of the array. Obviously the constraint would not apply at all to an array consisting of only a single element. Yet for an array of only five elements the center element clearly shows the predicted generic behavior. As one expects, when the number of elements in the array becomes larger, the effectiveness of the constraint increases. Figure 10 shows that even in an edge element the pattern is strongly modified in the direction predicted by the infinite-array model.

The element pattern may display relatively sharp dips or nulls. In the infinite-array model these may be classed as either necessary nulls or removable nulls [4]. The latter nulls are removable in the sense that a feed network exists which can in principle tune out these nulls. The location of necessary nulls in the element pattern is found on considering the operation of the antenna as a phased array. Such a null may occur in the direction indicated by the main lobe whenever a grating lobe just enters visible space (Appendix A). Figure 11a shows how this feature is effectively reproduced by the center element of a finite array of 25 elements. Again, even the edge element of the same array (Fig. 10b) shows the influence of this null, even though the infinite-array model cannot be expected to apply quantitatively near an array edge.

For closely spaced arrays the infinite-array constraints require zero radiation for certain excitations of the array. As has been stated, the general physical grounds for these constraints do not carry over to finite arrays. Thus the finite array can radiate (and can therefore in principle be matched) for all excitations. When this match is in fact attempted, that is, when the high degree of mismatch which replaces the absolute infinite-array constraint is tuned out, the correspondence with the infinite-array model is lost. This is illustrated by the element patterns shown in Fig. 12. In Fig. 12a only small mismatches are tuned out, whereas in Fig. 12d match for all excitations has been obtained in contradiction to the constraints of the infinite-array model. Figures 12b and 12c show various stages between these extremes. In Fig. 12d, as expected, correspondence with the infinite-array model is largely lost. In particular the element produces substantial radiation directed along the array. The generally unsatisfactory nature of this pattern commends acceptance of the constraints of the infinite-array model in setting design objectives for practical arrays.

The patterns shown in Fig. 11a suggest another application for suitably matched arrays. Appropriate placement of the necessary nulls synthesizes a pattern which is nearly constant interior to the nulls and is reduced by 5 dB in the region outside the null, vanishing along the array face.

ACKNOWLEDGMENTS

The author acknowledges constructive comments from Dr. T. L. ap Rhys and Mr. J. P. Shelton during the preparation of this report.

REFERENCES

1. J.L. Allen, "Gain and Impedance Variation in Scanned Dipole Arrays," *IRE Transactions on Antennas and Propagation* AP-10, 566–572 (Sept. 1962).
2. P.W. Hannan, "The Element-Gain Paradox for a Phased-Array Antenna," *IEEE Transactions on Antennas and Propagation* AP-12, 423–433 (July 1964).
3. W. Wasylkiwskyj and W.K. Kahn, "Element Patterns and Active Reflection Coefficient in Uniform Phased Arrays," *IEEE Transactions on Antennas and Propagation* AP-22, 207–212 (Mar. 1974).

4. W. Wasylkiwskyj and W.K. Kahn, "Element Pattern Bounds in Uniform Phased Arrays," Presented at URSI Fall Meeting, Boulder, Colorado, Oct. 1975; Digest Reference: Sessions VI-11, Arrays, p. 264.

5. W. Wasylkiwskyj and W.K. Kahn, "Efficiency as a Measure of Size of a Phased-Array Antenna," *IEEE Transactions on Antennas and Propagation* AP-21, 879-884 (Nov. 1973).

6. D.M. Sazonov and B.A. Mishustin, "Theory of Multibeam Antenna Arrays with Interacting Elements," *Radio Engineering and Electronic Physics* 13 (No. 8), 1186-1193 (1968).

7. D.E. Bergfried, "An Investigation of Transmission Through Linear Multiport Networks with Application to the Theory of Array Antennas," Dissertation for the degree Doctor of Science, The George Washington University, Washington, D.C., June 1973.

8. D.E. Bergfried and W.K. Kahn, "Impedance Matching of Phased Array Antennas for all Excitations by Connecting Networks," 1973 G-AP International Symposium, Aug. 22-24, Boulder, Colorado, Digest Reference: Session 20, Array Theory, pp. 124-126.

9. W.K. Kahn, "Efficiency of a Radiating Element in Circular Cylindrical Arrays," *IEEE Transactions on Antennas and Propagation* AP-19, 115-117 (Jan. 1971).

10. L.B. Felsen and W.K. Kahn, "Transfer Characteristics of 2*N*-Port Networks," pp. 477-512 in Proceedings of the Symposium on Millimeter Waves, P.I.B. Symposium Series, Vol. IX, 1959.

11. W. Wasylkiwskyj and W.K. Kahn, "Theory of Mutual Coupling Among Minimum-Scattering Antennas," *IEEE Transactions on Antennas and Propagation* AP-18, 204-216 (Mar. 1970).

12. W.K. Kahn, "Scattering Equivalent Circuits for Common Symmetrical Junctions," *IRE Transactions on Circuit Theory* CT-3, 121-127 (June 1956).

13. N. Amitay, V. Galindo, and C.P. Wu, *Theory and Analysis of Phased Array Antennas*, Wiley-Interscience, New York, Ch. 1, 1972.

14. G.V. Borgiotti, "A Novel Expression for the Mutual Admittance of Planar Radiating Elements," *IEEE Transactions on Antennas and Propagation*, AP-16, 329-333 (May 1968).

Appendix A

ELEMENT PATTERNS OF A MATCHED INFINITE ARRAY

A single element of an infinite planar lattice of identical elements is excited by a unit incident wave. The remaining elements (or their corresponding ports at the input to an interconnecting feed network) are terminated. The feed network has been adjusted or tuned so that, if all elements were excited with uniform amplitude and linear progressive phase, the array would be matched at all scan angles. The element pattern produced under these conditions was found in Ref. 4. A simplified planar array may be constructed as a linear array of sources, each of which has an infinite extent in the direction normal to the array axis. For this special case the resulting element pattern is given by

$$\hat{P}(\theta) = \frac{D_x}{\lambda} (\cos\theta) \left[1 + \sum_{m \neq 0} \frac{P(\theta_m)}{P(\theta)} \left(\frac{\cos\theta}{\cos\theta_m} \right) \right]^{-1} , \tag{A1}$$

where

$\hat{P}(\theta)$ = the limiting element pattern in the terminated-array environment obtained when the array is matched,

$P(\theta)$ = any element pattern in an arbitrarily terminated environment such as, e.g., the pattern of a single excited element of the original (unmatched) array when all other elements are open-circuited,

θ = pattern angle measured from the z axis (in the xz plane), $\theta \equiv \theta_0$,

θ_m = grating-lobe pattern angle defined by the equation

$$\sin\theta_m = \sin\theta - m\frac{\lambda}{D_x}, \qquad m = \pm 1, \pm 2, \ldots, \tag{A2}$$

D_x = spacing along the x axis, and

λ = wavelength.

The summation in Eq. (A1) extends over all real angles θ_m, $m = \pm 1, \pm 2, \ldots$, that is, those values of m, $m \neq 0$, such that

$$\left| \sin\theta - m\frac{\lambda}{D_x} \right| \leqslant 1 . \tag{A3}$$

The most significant feature of Eq. (A1) resides in the singularities of the term

$$\sum_{m \neq 0} \frac{P(\theta_m)}{P(\theta)} \frac{\cos \theta}{\cos \theta_m} . \tag{A4}$$

The ratios $P(\theta_m)/P(\theta)$ are shown to be invariant, that is, the same for *any* element pattern of a given antenna element independent of termination or (uniform) interconnecting feed network. Each singularity of (A4) corresponds to a necessary null of the element pattern in the terminated-array environment.